JOURNAL OF OPTOELECTRONICS AND ADVANCED MATERIALS Vol. 12, No. 11, November 2010, p. 2288 - 2295

Study of the conduction mechanisms in poly-perfluoro-sulfonated membranes impregnated with intrinsic semiconducting polymers

A. ANDRONIE[*], S. ANTOHE[a], S. IORDACHE, A. CUCU, S. STAMATIN, A. CIOCANEA[b], A. EMANDI[c], G. NAN[d], C. BERLIC[d], G. A. RIMBU[e], I. STAMATIN

University of Bucharest, Physics Department, 3Nano-SAE Research Centre, P.O.Box MG-38, 077125 Magurele, Bucharest-Romania

[a]*University of Bucharest, Faculty of Physics, Mat&Devices Elect&Optoelctr Center, P.O. Box MG-11, 405 Atomistilor Str., 077125, Magurele, Romania*

[b]*Polytechnica University of Bucharest, 313 Splaiul Independenței, 060042, Bucharest, Romania*

[c]*University of Bucharest, Faculty of Chemistry, Department of Inorganic Chemistry, 23 Dumbrava Rosie Str., RO-010184 Bucharest, Romania*

[d]*University of Bucharest, Faculty of Physics, P.O. Box MG-11, 405 Atomistilor Str., 077125, Magurele, Romania*

[e]*INCDIE ICPE-CA, 313 Splaiul Unirii, P. O. Box 149, Bucharest 030138, Romania*

Electrical conduction mechanisms for poly-perfluorosulfonated membranes with intrinsic conducting polymers (ICP) insertion were investigated as function of relative humidity (RH) at 80^{0}C. Polyaniline, polypyrrole, polythiophene were in situ polymerized using an appropriate couple: monomer-solvent- oxidant. Two mechanisms were identified for the electrical conduction which are dependent of the relative humidity: dissociative- from the sulfonic group contribution and hopping-migration through the water phase. ICPs with electronic conduction induced by polarons and electron inter-chain hopping have a minor influence on the ionic conduction due to the water interlayer between hydrophobic polymer and hydrophilic perfluorinated matrix. The exception observed is the polypyrrole- polyperfluorosulfonated membrane which led to constant 90-100 mS/cm conductivity not depending on relative humidity. The thermal stability and degradation were investigated by differential scanning calorimetry and thermogravimetric analysis. ICP modified membranes showed an improvement of the onset decomposition temperature from 290^{0}C to 350- 370^{0}C depending on ICP polymer type.

(Received October 14, 2010; accepted November 19, 2010)

Keywords: Perfluorosulfonated membranes, Intrinsic conducting polymers, Conduction mechanisms

1 Introduction

Fuel cell membranes are usually made of electrochemical active polymers where proton conduction is dominant. Perfluorosulfonated materials in acidic form (PFSA) under registered mark such as Nafion, Aciplex, Flemion, Hyflon, Dow [1-4] are representatives for this class. The proton conduction is dependent of the hydration level and the mechanisms are in agreement with the model developed by Grotthuss (proton hopping through hydrogen bonded network of the water molecules) or by migrating/diffusion phenomenon of hydrated proton $[H^+(H_2O)_n]$ species [5,6]. A more complex model based on "structural diffusion" and cooperative processes was developed assuming H_5O^{2+} complex structure with low mobility and hopping activation energy [7, 8, 9]. These species are formed only in hydrated PFSA where $-HSO_3$- pendant groups define small void clusters (microdomains) filled with water molecules. At high hydration level, these microdomains increase in dimension ("swell") developing a network of interconnected micro-channels with water molecules within the polymer matrix. The electrical conductivity is governed by protons resulted from dissociative and migration processes. Such processes occur in microdomains volume and at their interfaces and they are dependent on percolation and phase inversion thresholds. The percolation, similar to the phenomenon encountered in a polymer matrix filled with small particles [10, 11], takes place at moderate hydration level, while phase inversion occurs at higher hydration level. The microdomains structure was rigorous studied by NMR revealing reversible micellar membranes when swollen with water or ethanol [12]. In dry form, the thickness of the microdomains delimited by pendant groups was found to be about 3.8-4 nm, with a ~10 nm periodicity. The addition of 20 wt % water induces a domain swelling up to 7 nm without any change in overall periodicity. The addition of 20% wt ethanol determines an increase of the microdomains to 11 nm with a periodicity of 19 nm, phenomenon assigned to morphological reorganization. The topography obtained by atomic force microscopy (AFM) confirms the reverse micellar model for Nafion 117 [13]. For dry membrane, under ambient humidity conditions, microdomains size ranged between 4 and 10 nm. A 50% bulk swelling in deionized water determines a rise up to 7-15 nm of the microdomains interconnected by

microchannels developed an ion rich phase. X-ray diffraction, small angle x-ray scattering and neutron scattering [8, 14, 15] add new information on the structural evolution of perfluorosulfonated membranes with the hydration level. The maximum scattering or "ionomer peak" was observed up to large water contents of 65 wt.%, with a phase inversion at 50 wt.% (Perfluorosulfonated ionomer membranes with high water contents were formed by placing the membranes in water at 120°C for a few hours). A proposed model assumes sulfonic acid domains as cylindrical pores with sulfonic acid groups on the pore edges surrounded by an unsulfonated matrix until the water content reaches 50 wt.%. At this point, a phase inversion occurs when the unsulfonated matrix is no longer continuous and sulfonic acid groups reside on the outside of rod-like micellar structures and the membrane is fully plasticized. The electrical conductivity measurements have shown strong influence on the water content. Values of 100mS/cm were reported by Electrochemical Impedance Spectroscopy in 1-100 KHz range on Nafion series [16, 17, 18] in fully hydrated state, that is, the maximum number of water molecules per sulfonic group up to 20–22.

The main approach in improving conductivity performances related to other characteristics (life cycle, mechanical stability, cross over effects by water /methanol electro osmosis, etc) focused on impregnation with additives such as: silica, phosphates, limes, ionic liquids, conductive and electroactive polymers [8, 19, 20, 21]. As regarding conductive polymers, the attention was focused on polyanilines (PANi) and polypyrroles (PPY) due to their high conductivity induced by doping or as intrinsic conductive polymers (ICPs) resulted by appropriate polymerization. PANi was deposited as an intermediate layer for catalyst activity improvement, CO poisoning and methanol crossover effect reduction. When PANi is polymerized within membranes, due to its insolubility in water, a hydrophobic phase takes place with reciprocal rearrangement of hydrophobic polymer backbone and hydrophilic pendant groups [19, 20]. Unfortunately low aniline monomer solubility in water makes it not appropriate direct polymerization into PFSA membranes. Polypyrrole has the same influence as hydrophobic phase [20] with the advantage that the monomer is soluble in water and, therefore, the polymerization can be performed into membrane microdomains. A similar attempt in obtaining an improved ionic conductivity and high power density was performed by poly thiophene incorporation (PTH) in Nafion 117 membranes [22], but the effect on the ionic conductivity has not been clearly observed. ICPs have different influences on the conduction mechanisms in PFSA. Polymers with redox states and those with electrical conduction controlled by polarons or bipolarons (PANi, PPY, PTH) or as n-doped in oxidized state are expected to have a determinant role in proton conduction mechanisms [23, 24, 25].

A series of experiments were performed by insertion into PFSA matrix for emphasizing the role of each electronic polymer class, related to thermal behaviour and proton conduction mechanisms. The following assumptions were made: 1. PFSA are ion-exchange polymers containing electrostatic bounded redox centers with capacity to incorporate a series of electroactive or intrinsically conductive polymers [25]; 2. Intrinsic conducting polymers (ICPs) are mainly hydrophobic and conduction mechanisms in the presence of counterion develop a charge delocalization (polarons and bipolarons) which could amplify the proton mobility [23, 24, 25]. This contribution takes into account only ICPs which can be incorporated into PFSA matrix starting with appropriate monomers for in situ polymerization resulting in PANi, PPY, PTH. Thermogravimetric analysis (TGA) and differential scanning calorimetry (DSC) were used to evaluate thermal stability and phase transformations induced by ICPs insertion into PFSA matrix. Electrical conductivity was measured as function of humidity at constant temperature (80^0C) using an in-plane four point cell. Two types of solvents are considered, water and 40wt% ethanol-water for establishing their influence on the electrical conductivity.

2 Experimental

2.1. Materials

Membranes: PFSA membrane: grade Fumapem 1050, supplier FuMA-Tech GmbH (Equivalent weight EW=1000 g/eq, specific conductivity in acidic form >85 mS/cm, water uptake 25wt% at room temperature, thickness 50-60 microns, dimensional swelling in water at 80^0C, 7%, density 1.98 - 2 g/cm, glass transition, 110^0C, temperature of start thermal decomposition 270-300^0C).

Monomers: Aniline sulfate monohydrate (SA) and 2,5 anilinium disulfate monohydrate (DSA), Sigma Aldrich, grades for chemical analysis. Pyrrole and Thiophene (monomers for chemical analysis, purchased from Sigma Aldrich, grades for chemical analysis) were distilled and used as fresh distilled fraction in polymerization.

Oxidants: Amonium peroxidislulfate (APS) for SA and DSA; Iron (III) p-toluene sulfonate tertahydrate (FePTS) for pyrrole and thiophene (Both are chemical grade for analysis, Sigma Aldrich).

Solvents: Bidistilled and demineralised water, 40% wt ethanol 100%-water.

2.2. Preparation of membranes with ICPs

Fumapem F1050 in salt form was treated in 10% aqueous solution of HNO_3 for 3h at 90^0C.

Table 1. Electronic conductivity and conduction mechanisms for ICPs.

Monomer-oxidant	Polymerization media	σ (S/cm)	Conduction mechanism	Ref
Aniline-APS	Aqueous sulfuric acid	10-15	Intrachain: electronic, polaron Interchains:hopping- σ decreases with temperature	[36]
Pyrrole- p-toluenesulfonate Salts	Aqueous solution	500	Intrachain: polaron, bipolaron, metallic conductivity	[38]
Pyrrole-other oxidants	Aprotic solvents, aqueous solutions	0.1-100	Intrachain: electronic, polaron Interchains:hopping σ decreases with temperature	[37]
Thiophene-FeCl3	Acidic solutions	10-100	Intrachain: electronic, polaron Interchains:hopping (Mott) σ decreases with temperature	[40]
Thiophene-FepTS-	Acidic solutions	500	Metallic conductivity	[39]

After washing with demineralised water the membranes were boiled for 1 h at 90^0C. Finally the membranes were washed with demineralised water (~pH 7) and kept in 0.5M H_2SO_4 solution. Before immersion in monomer solution PFSA, F-1050 was dried at 80-85^0C. Modified membranes were obtained by impregnating F-1050 membranes with the appropriate ICP, using monomers and oxidants as follows: F-1050SA- the monomer SA in water solvent, oxidant APS; F-1050DSA- the monomer DSA in water solvent, oxidant APS; F-1050PYW- the monomer pyrrole in water solvent, oxidant FePTS; F-1050 PYE- the monomer pyrrole in water-40% ethanol solvent, oxidant FePTS; F-1050THW- the monomer thiophene in water solvent, oxidant FePTS; F-1050THE- the monomer thiophene in water-40% ethanol solvent, oxidant FePTS. Each F1050 membrane conditioned and dried at 80-85^0C was immersed in 25 ml of 0.2M monomer in appropriate solvent for 1h. Separately, a 0.2 M solution of appropriate oxidant was prepared in the same monomer solvent. Then, a quantity of 10ml oxidant solution was added in drop wise for 1h under stirring at RT. The polymerization process continued for 4 h under stirring. Finally the samples were removed, washed with distilled water in order to remove by-products and oxidants and kept at RT.

2.3. Characterization methods

Thermal analysis. Thermal analysis are performed by means of differential scanning calorimeter (DSC Mettler Toledo, model Star1) in nitrogen at a heating rate of 10^0C/min in range 25-400^0C. The 5-10 mg samples are sealed in aluminum pans. DSC curves were analyzed with DSC Standard Data Analysis Program associated with model Star1. Thermogravimetric analysis (TGA/SDTA Mettler Toledo) was performed in air at a heating rate of 5^0C/min in the range 25-400^0C. Before measurements, all membranes were conditioned at RT for 24 h.

Polymer content. Dried F-1050 membrane kept at 85^0C for 12h was used as reference. The ICP modified membranes were measured after drying in the same conditions as the reference membrane. Polymer content was measured by:

PC[%]=(dry sample with polymer- dry F1050 membrane)/dry F1050 membrane

Conductivity. The conductivity was measured via four-point BekkTech conductivity test cell (BT-512 Membrane Conductivity Test System, Bekktech LLC, USA) at a set point temperature of 80^0C. Membrane samples were cut into strips of approximately 15 mm length and 4-5 mm wide and placed in the four-point probe cell (distance between middle electrodes, 4.2 mm) with temperature and humidity (± 1 degree absolute accuracy) controlled in nitrogen gas by a back-pressure regulator [26]. Conductivity testing is a good solution because contact resistance and catalyst effect are eliminated when measurements are taken on the membrane electrode assembly. In addition this method gives information regarding the type of charge carriers when composites or other electronic conductors are inserted in the polymer matrix.

3. Results and discussion

3.1 Polymer content

The polymer content is strongly dependent on monomer-solvent couple (Fig. 1). The monomer has a major influence when water is the solvent. For anilines in sulfate and disulfate form, due to electrostatic interactions between $-HSO_3$ pendant groups and sulfate, the quantity of monomer increases slowly with the number of sulfate groups per aniline. Pyrrole and thiophene have a higher swelling capacity close to double respective triple capacity to be inserted in perfluorosulfonated membranes. In consequence, the quantity of polymers in the membrane microdomains increases in considerable amount. On the other hand, ethanol has a high swelling capacity for PFSA leading to a larger amount of absorbed monomers than in the case of water.

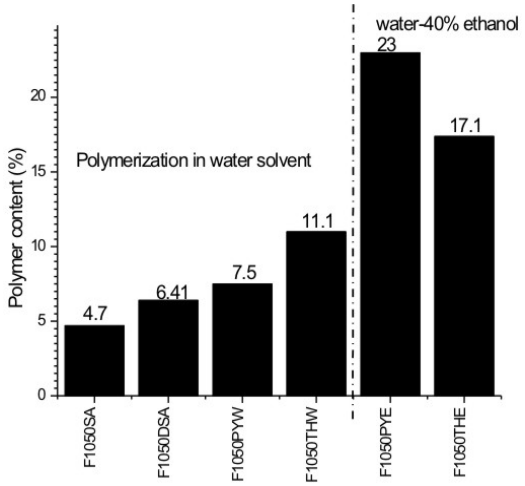

Fig. 1. ICP content of modified PFSA membranes measured for dry membranes before and after in situ polymerization.

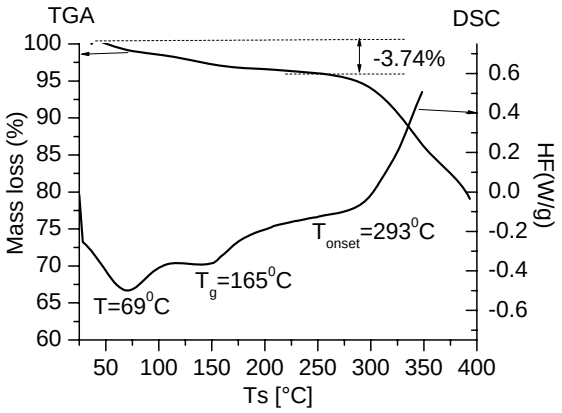

Fig. 2. Thermal stability and transformations induced by water loss for Fumapem F1050 in acidic form conditioned at RT- TGA and DSC (^exo) curves. Two glass transitions are indexed at 110°C (in the shoulder of the water loss valleys) assigned to acidic form, respectively 165°C assigned to the dry form.

Therefore, polypyrrole content in F1050PYE is 3.06 times higher than in F1050PYW case and polythiophene content in F1050THE is 1.54 times higher than in F1050THW. Due to the low solubility of aniline sulphates in ethanol, the polymerization process has not been successfully accomplished when ethanol was used as solvent. Moreover, aniline monomer is not appropriate to be inserted in polymer matrix due to its low solubility in water and specific conditions for polymerization (strong aqueous acids at low pH <2, where in the intermediate stage is converted first in sulphate) [25].

3.2 Thermal behaviour of PFSA- conducting polymer systems

Thermal behaviour of F1050 in acidic form is shown in Fig. 2, where few specific features are distinguished: 1. on DSC curve, the endothermic valleys with minimum at 69°C assigned to water desorption accompanied by conformational reorganization of macromolecular chains, corresponding to a small mass loss of 1.85% on TGA curve; 2. the glass transition at 165°C (midpoint) is assigned to the dry form of the membranes, namely, to tetrafluoroethylene backbone of PFSA membranes [27]. A second glass transition at about 110°C shadowed by water desorption valley at the right shoulder is assigned to F1050 acidic form (glass transition behaviour of perfluorinated polyionomers was intensely studied [28, 29]); 3. The start decomposition temperature is indexed in the same 293-295°C range on both TGA and DSC curves. On TGA curve, a continuous mass loss of about 1.9% is observed, due to residual/bounded water loss or/and very weak dehydrogenation of the $-HSO_3$ pendant groups. In ICP modified membranes, thermal effects are dependent on the monomer- solvent couple, respectively, on the number of sulphate groups in aniline monomers.

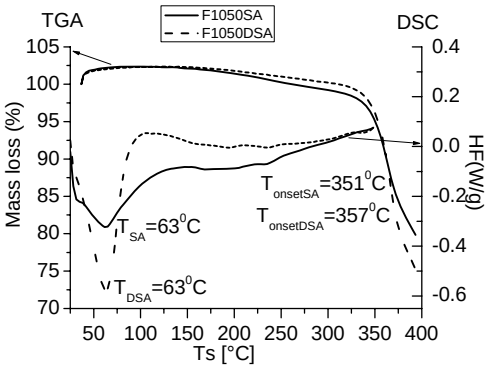

Fig.3. Thermal stability and transformations induced by polyanilines in situ polymerized from anilinium sulphate (F1050SA) and anilinium disulfate (F1050DSA) - TGA and DSC (^exo) curves.

For F1050SA and F1050DSA, TGA curves show a mass loss of 3.7%, respectively 2.7%, with the start temperature of decomposition increased to 351°C and to 357°C (Fig. 3). As concerning the total mass loss, F1050SA is similar to F1050, while in F1050DSA a small improvement can be observed. It can be concluded that there is an increase in hydrogen bounding between sulphate groups and $-HSO_3$ pendant groups. On DSC curves, by comparison with Fig. 2, water desorption associated with conformational changes is close to half of the corresponding value for F1050SA and double for F1050DSA. The first glass transition can be appreciated in range 80-90°C for F1050SA and 110-120°C for F1050DSA. Small exothermic effects are observed at temperatures over 240°C, but down to the starting decomposition temperature there are no changes. Thermal stability of polyanilines determined by the backbone

degradation was reported to be in the range of 350-500^{0}C depending on dopant [30].

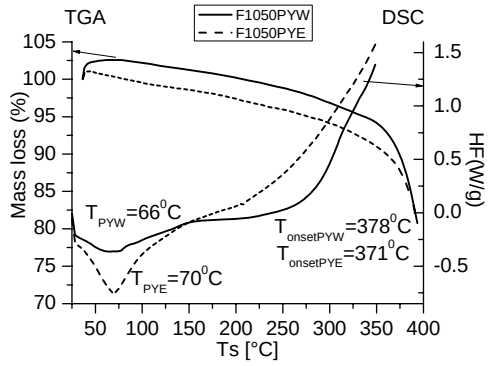

Fig. 4. Thermal stability and transformations induced by polypyrroles in situ polymerized using water as solvent (F1050PYW) and 40% ethanol in water (F1050PYE)- TGA and DSC (^exo) curves.

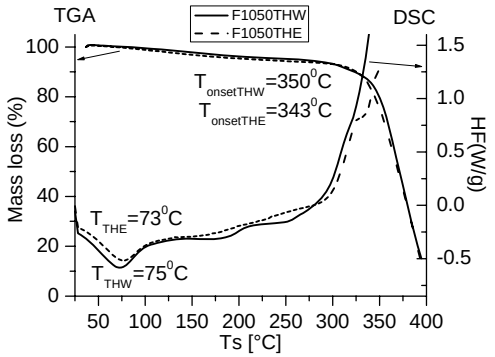

Fig. 5. Thermal stability and transformations induced by polythiophenes in situ polymerized using water as solvent (F1050THW) and 40% ethanol in water (F1050THE)- TGA and DSC (^exo) curves.

We can conclude that there is an improvement in thermal stability induced by polyanilines, but it is not dependent on the number of sulfate groups in the initial monomer. Similarly, polypyrrole and polythiophene based compounds show an improved thermal stability, but with a continuous mass loss up to the starting decomposition temperature.

On TGA curves, there is a slight dependence on solvent (ethanol or water). Polypyrrole extends the range of thermal stability up to 371-378^{0}C (Fig. 4) and polythiophene up to 343-350^{0}C (Fig. 5). On DSC curves, thermal decomposition is revealed at much lower temperatures depending on polypyrole solvent. For polypyrrole in water solvent, the thermal effect of the backbone degradation starts at 280^{0}C and for ethanol at 244^{0}C. In case of polythiophene, there are similar solvent effects, but at higher temperatures (299^{0}C for water and 288^{0}C for ethanol). These phenomena supply useful information with regard to polymer structural organization into membrane microdomains with impact on the electrical conductivity mechanisms. Thermal stability of the polypyrroles as reported in [31] is 200-300^{0}C in nitrogen atmosphere with a continuous mass loss of 15% function of doping agent. In addition, polypyrrole and polythiophene thermal stability studies establish the same characteristics for both polymers marking two steps of degradation reactions which involve dopant loss and, then, polymer backbone degradation [32]. On DSC curves (Fig. 4) two transformation stages are evidenced, with a slight change in inflexion for F1050PYW at 320^{0}C (Fig. 4) and more obvious for polythiophenes at 310^{0}C (F1050PTHW) respectively 320^{0}C (F1050PTHE) on Fig. 5. TGA curves show mass loss over 340^{0}C for all polymers inserted in membranes. Based on these effects, we can conclude that the polymerization process is strongly influenced by –HSO_3 pendant groups which participate at self-doping and bonding to the polymer backbone, resulting in a specific stereoregularity. A structural model can be elaborated taking into account the above mentioned phenomena: 1. H-N= in pyrrole aromatic rings bonds to –HSO_3 pendant groups leading to a polymer with high isotacticity. For thiophene, H-S= groups are involved, but the bonding to –HSO_3 is stronger as observed on DSC curves (Fig. 4 and 5). In the case of polyanilines, where the interaction between sulfate and –HSO_3 groups is dominant, a specific conformation is induced for a typical ladder polymer. 2. Polymer degradation starts with backbone fracture resulting in fragments which remain bonded to the PFSA matrix and released later once the temperature increases. Structural organization of the polymer within F1050 matrix is strongly influenced by the monomer type and it is observable by glass transition and water desorption valley evaluation. For polypyrrole, we have only the first glass transition at 130 and 138^{0}C for both solvents, while for polythiophene only the second glass transition at 200^{0}C for water and 217^{0}C for ethanol is shown. Moreover, sulfonic groups from perfluorosulfonated polymer play a counterion role for the polymer backbones and, therefore, they influence the development of polaron charges which are spatially modulated function of distribution and orientation of -HSO_3 pendant groups.

3.3 In-plane electrical conductivity

The electrical conductivity measured at fixed temperature (80^{0}C) has a specific dependence on relative humidity (RH) for each monomer-solvent-oxidant couple. Electrical conductivities for all samples are shown in Fig. 6. By comparison to F1050, considered pure ionic conductor, polymer and solvent dependent behaviour are clearly evidenced. PFSA –F1050 conductivity increases with RH reaching its maximum value of ~140mS/cm when fully hydrated. In log plot function of RH (Fig. 7), three distinct regions are evidenced, defined by RH =30% and by RH=80%, where conduction mechanisms change. The determinant parameter is the number of water moles, nH_2O, in the system at a given volume and temperature. On the other hand, $\lambda = nH_2O/nSO_3H$ (number of moles of water per equivalent of polymer or by the number of

sulfonic groups) [33, 34] is the parameter related to a structure having the physical properties of a poly-ionomer.

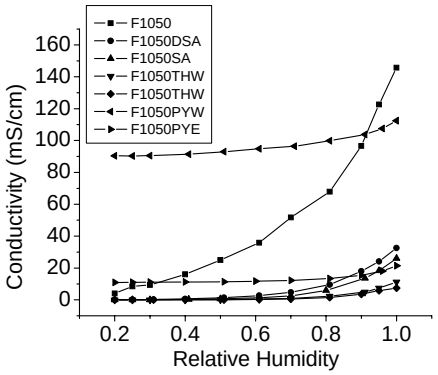

Fig. 6. Electrical conductivity, measured by in plan four points method, as function of the relative humidity for a fixed temperature of 80 ^{0}C.

A linear equation for parameters λ and RH can be assigned: $\lambda(RH)=a*RH*P_{H2O}(T)$, with a- constant and $P_{H2O}(T)$- the saturated vapour pressure at mixture temperature (in our experiments nitrogen-water vapours). As we see in Fig. 7, the logarithm of conductivity has a linear dependence on humidity for three distinct regions, which can be directly associated with the λ parameter: $log\sigma=a+\beta\lambda(RH)$, where β (dimensionless parameter) is the slope of the linear curve and it is straightforwardly connected to the conduction mechanisms issued in different models.

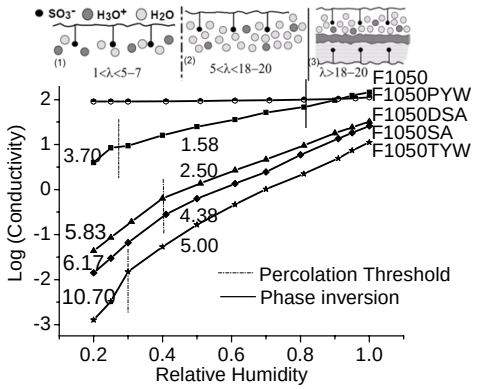

Fig. 7. Log plot of the electrical conductivity vs relative humidity for ICPs inserted in PFSA using water solvent. For PFSA and ICPs inserted in PFSA, three regions are identified assigned to percolation (RH= 30-40%), middle region up to RH=80% and phase inversion. For each region one dominant conduction mechanism is associated dependent on the number of water molecules per sulfonic group: (1) dissociative with proton hopping, (2) dissociative with hydrated proton diffusion/migration, (3) equal dissociation and migration rates and plasticized PFSA matrix.

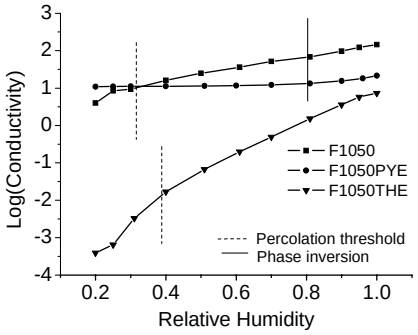

Fig. 8. Log plot of the electrical conductivity vs relative humidity for ICPs inserted in PFSA using 40% ethanol-water solvent.

If a maximum hydration level of 80% RH (F1050, Fig. 7) corresponds to λ =16-20 water molecules per sulfonic group [34, 35], then, at 30% RH, the value for λ ranges from 1 up to 5-7 molecules per sulfonic group. In the percolation region up to RH=30%, a slope of 3.7 is assigned to dissociative processes with the proton hopping along "–$HSO^{3-}H^{3+}O^{-}H_2O$-"chains (Fig. 7, mechanism (1)) in PFSA microdomains. In the middle region, the conductivity increases quasi linearly with RH. The conduction is governed by two competitive processes defined by the dissociative rate and by the migration rate of hydrated proton (Fig. 7, mechanism (2)). The slope of 1.58 shows that the dissociative rate is greater than the migration rate. When both rates are equals, the phase inversion takes place (RH=80%, λ=16-20 water molecules per sulfonic group) and the polymer matrix plasticizes (mechanism (3) in Fig. 7). A slightly increasing conductivity can be assigned to other dissociative processes due to excess water molecules mediated by sulfonic pendant groups. If we take into account the structural models [8, 34, 35] for PFSA as nano-phase-separated materials, the ionic conduction is the result of proton dissociation from acidic sites (-SO_3H pendant groups) in the presence of confined water in hydrophilic domains. The dissociated proton is transferred to the water environment and transported through the membrane. At low hydration level, the conduction mechanism is defined by proton hopping between acidic sites mediated by water molecules until percolation threshold is reached (consider here the maximum value and not the initial threshold as usually defined in the percolation theory). Above percolation threshold, diffusion and migration mechanisms are dominant, being strongly dependent on water molecules confined in the hydrophilic domains. When considering ICP doping role, it is expected to obtain an electronic contribution or charge compensation in the electrical conductivity. Summarizing literature data (Table 1) for ICPs polymerized in similar experimental conditions, we observe a high electronic conductivity, where all ICPs exhibit electronic conductivity reaching a metallic state function of doping and oxidant. Nevertheless, ICPs inserted in PFSA matrix significantly

decrease the magnitude of electrical conductivity with the exception of polypyrrole in water solvent. A lower conductivity at low RH can be associated with charge compensation due to polymer bonding to sulfonic groups mediated by hydrogen bonds. With RH increasing over the percolation threshold, the electrical conductivity significantly increases but at much lower values than F1050. In Fig. 7, the slopes in the region up to percolation threshold are higher than for F1050 case. The reason could be that the dissociative rate increases with water content, but the proton is either compensated by the electronic charge from ICPs or/and proton migration is attenuated due to a small amount of water molecules. Clearly, with increasing sulphates on polymer backbones, there is no significant improvement (F1050SA and F1050DSA, Fig. 7). Polythiophene (F1050THW) gives rise to higher charge compensation decreasing the proton conductivity. Here, polythiophene shows a typical S-shape transition in the percolation region for both solvents (F1050THW- Fig. 7, F1050THE-Fig.8). In the middle region, the phenomena are similar to those taking place in F1050 with a superimposed effect of charge compensation more or less attenuated by the type of polymer. With water content increasing and taking into account polymer hydrophobicity, a continuous separation between ICP and PFSA takes place until the water forms a separation layer and hydrated protons are less compensated by the electronic charge. The exception is the polypyrrole which has a different behaviour. The electrical conductivity has a very low dependence on RH in the whole range, without percolation and phase inversion. F1050PYW (Fig. 7) maintains a 90-100 mS/cm constant high value of the conductivity. Unfortunately, it could not be established if, in polypyrrole case, there is proton or electronic conduction. For ethanol- water solvent, the electrical conductivity is reduced by a factor of 10 for polypyrrole (F1050PYE, Fig. 8) with a very slow dependence of RH. The polythiophenes polymerized in membranes with ethanol-water solvent also decreases the electrical conductivity (F1050THE, Fig. 8). The transition to percolation threshold is continuous up to 40% RH. The slope in the middle region is 5.3 and the maximum value of the conductivity is around 5-10 mS/cm at RH=80% for either water or ethanol- water solvent.

4. Conclusions

Conduction mechanisms in perfluorosulfonated polymers are defined by dissociative processes on sulfonic pendant groups with transport by hopping and migration of the hydrated protons function of the hydration level. Intrinsic conducting polymers impregnated in PFSA membranes, as a general behaviour, do not improve their ionic conductivity. The polypyrroles inserted in PFSA membranes rise to a constant value of the electrical conductivity independent of the hydration level. The ethanol-water solvent decreases the electrical conductivity. All ICPs have led to an improvement in thermal stability related to the start decomposition temperature, but there is an intrinsic degradation of the polymers before decomposition. ICP impregnated PFSA membranes have a strongly negative response to ethanol exposure and, therefore, alcohol crossover effects should be evaluated.

Acknowledgements

The authors acknowledge the financial support from POSDRU/6/1.5/S/10/2008, national projects Centres of Excellence (CEEX), CEEX 704, 760, X2C19, National Program PN-II, contract 11-024, 22-136/2008, the National University Research Council (NURC), Contract 222/2007, and NATO reintegration grants NATO-RIG 984214.

References

[1] Renaud Souzy, Bruno Ameduri, Prog. Polym. Sci. **30** 644 (2005)
[2] Carla Heitner-Wirguin, J. Membr. Sci. **120**, 1 (1996).
[3] P. Costamagna, S. Srinivasan, J. Power Sources **102** 242 (2001).
[4] A.E Steck, C. Stone, Membrane materials in fuel cells, 2nd Int. Symp. on New Materials for Fuel Cells and Modern Battery Systems, Montreal, Canada, July 1997, 792-807.
[5] T. Arimura, D. Ostrovskii, T. Okada, G. Xie, Solid State Ionics **118**, 1 (1999).
[6] G. Inzelt, M. Pineri, J. W. Schultze, M. A. Vorotyntsev, Electrochimica Acta **45** 2403 (2000).
[7] G. Zundel, J. Membr. Sci. **11** (1982) 249.
[8] Kenneth A. Mauritz, Robert B. Moore, Chem. Rev. **104**, 4535 (2004).
[9] B. Smitha, S. Sridhar, A.A. Khan J. Membr. Sci **259**, 10 (2005)
[10] Yong Wu, B. Schmittmann, R.K.P Zia, J. Phys. A: Math. Theor. **41**, 025004 (2008)
[11] R. K. P Zia, Yong Wu, B. Schmittmann, J Mathematical Chemistry, **45**, 58 (2009).
[12] G. Meresi, Y. Wang, A. Bandis, P.T. Inglefield, A. A. Jones, W-Y. Wen, Polymer **42,** 6153 (2001).
[13] McLean, R.S. M. Doyle, B.B. Sauer, Macromolecules **33**, 6541 (2000).
[14] G. Gebel, Polymer **41**, 5829 (2000).
[15] M. Laporta, M. Pegoraro, L. Zanderighi, Macromolecular Materials and Engineering **282**, 22 (2000).
[16] T. A. Zawodzinski, M. Neeman, L.O. Sillerud, S. Gottesfeld, J. Phys.Chem. **95,** 6040 (1991).
[17] Y. Sone, P. Ekdunge, D. Simonsson, J. Electrochem. Soc. **4**, 1254 (1996).
[18] R. F. Silva, M. De Francesco, A. Pozio, Journal of Power Sources **134,** 18 (2004).
[19] Vladimir Neburchilov, Jonathan Martin, Haijiang Wang, Jiujun Zhang, Journal of Power Sources **169,** 221 (2007).
[20] F. Xu, C. Innocent, B. Bonnet, D.J. Jones, J. Roziere, Fuel Cells **5,** 398 (2005).

[21] A. Andronie, S. Antohe, S. Iordache, S. Stamatin, A. Cucu, A. Ciocanea, A. Emandi, E. Ur, I, Stamatin, Optoelectron. Adv. Mater. Rapid Comm. **4**(11) 1807, (2010).
[22] B. Tazi, O. Savadogo, Journal of New Materials for Electrochemical Systems **4,** 187 (2001).
[23] G. Inzelt, Conducting Polymers a New Era in Electrochemistry, Springer (2008)
[24] T. A Skotheim, J.R. Reynolds Eds, Handbook of Conducting Polymers, 3rd Ed, Conjugated Polymers Processing and Applications, CRC Press, Taylor & Francis (2007)
[25] Gordon G. Wallace, Geoffrey M. Spinks, Leon A.P. Kane-Maguire, Peter R. Teasdale, Conductive Electroactive Polymers. Intelligent Polymer Systems, 3rd Ed,CRC Pres,(2009)
[26] www.bekktech.com
[27] G. G. Hougham, P. E. Cassidy, K. Johns, T. Davidson, (Eds.) Fluoropolymers 2: Properties, Series: Topics in Applied Chemistry, XVII, Springer (1999)
[28] Swee Chye Yeo, A. Eisenberg, J. of Applied Polymer Science **21,** 875 (2003).
[29] J. J. Fontanella M. C. Wintersgill, R. S. Chen, Y. Wu, S. G. Greenbaum, Electrochimica Acta **40,** 2321 (1995).
[30] Reza Ansari, M. B. Keivani, E-Journal of Chemistry, **3**, 202 (2006).
[31] P. Syed Abthagir, R. Saraswathi, Materials Chemistry and Physics **92,** 21 (2005).
[32] F. Mohammad, P. D. Calvert, N. C. Billingham Bull. Mater. Sci. **18**, 255 (1995).
[33] S. J Paddison, Annual Rev Materials Research, **33,** 289 (2003).
[34] T. A. Zawodzinski, C. Derouin, S. Radzinski, R. J. Sherman, Van T. Smith, T. E. Springer, S. Gottesfeld, J. Electrochem. Soc. **140**, 1041 (1993).
[35] A Gruger, A Regis, T. Schmatko, P. Colomban, Vibr. Spectroscopy, **26,** 215 (2001).
[36] Jan Prokes, Jaroslav Stejskal, Polymer Degradation and Stability **86,** 187 (2004).
[37] P. Syed Abthagir, R. Saraswathi, Materials Chemistry and Physics **92,** 21 (2005).
[38] A.F. Diaz, K.K. Kanazawa, G.P. Gardin, J. Chem. Soc., Chem. Commun, 635 (1979).
[39] L. Groenendaal, F. Jonas, D. Freitag, H. Pielartzik, J. R Reynolds, Adv Mater **12**, 481 (2000)
[40] K. Kobayashi, J. Chen, T.C. Chung, F. Moraes, A. J. Heeger, F. Wudl, Synth. Met. **9**, 77 (1984)

*Corresponding author: office@3nanosae.org